Assessment of pore collapse in North Sea Lover Cretaceous carbonates using downhole elastic strain

IDA L. FABRICIUS & LEONARDO T. P. MEIRELES

Geological Society of Denmark
https://2dgf.dk

Received 19 December 2024
Accepted in revised form 1 May 2025
Published online 13 May 2025

© 2025 the authors. Re-use of material is permitted, provided this work is cited. Creative Commons License CC BY: https://creativecommons.org/licenses/by/4.0/

Fabricius, I.L. & Meireles, L.T.P. 2025. Assessment of pore collapse in North Sea Lover Cretaceous carbonates using downhole elastic strain. Bulletin of the Geological Society of Denmark, Vol. 71, pp. 115–125. ISSN 2245-7070. https://doi.org/10.37570/bgsd-2025-71-07

The potential for pore collapse is a concern when producing hydrocarbons from fragile sedimentary rocks, like chalks. The reason is that although pore collapse can be a valuable drive mechanism, it can also cause large scale compaction and surface subsidence. This risk is as a rule evaluated from results of rock mechanical testing of core samples, but because a given reservoir typically comprises layers of different porosity, the stress required for fracturing or pore-collapse is then generalized as a function of porosity. Due to different diagenetic history, different reservoirs can have different degree of cementation (induration) for a given porosity, so each reservoir requires a separate stress-porosity relationship.

Recent studies of chalk indicate that pore collapse happens at a critical elastic strain irrespective of porosity, pore fluid, and induration. This should not be surprising, bearing in mind that the strain of the rock represents an equal strain of the mineral crystals constituting the rock frame, so that onset of pore collapse in chalk is governed by the *in situ* elastic strain of the calcite. Chalk can be rich in minerals like clay or quartz, but when calcite constitutes the frame, it is calcite that is elastically strained. The simple point is that elastic strain of the calcite crystals is the same as the elastic strain of the rock.

A complication with rock mechanical data is that the tested material has been brought to the surface by coring, a process that typically causes tested rocks to contain microcracks (small unloading fractures), so that the tested rocks do not truly represent the rock *in situ*. This issue points to using downhole deformation data, but these are sparse. A possibility is then to use information from geophysical well logs, because *in situ* elastic strain can be calculated from well log data, so that the results from rock mechanical testing can be generalized in a simple way. The method for strain calculation is here applied to data from the Valdemar field, which produces hydrocarbons from the Tuxen and Sola formations, a clay-rich Lower Cretaceous chalk interval in the Central North Sea.

Key words. Aptian, Barremian, Cretaceous, chalk, marlstone, rock physics, pore collapse, small strain

Ida L. Fabricius [ilfa@dtu.dk] and Leonardo T. P. Meireles, Department of Environmental and Resource Engineering, Technical University of Denmark, Denmark. *present address: [LETE@equinor.com]*

Already at a relatively early stage, production of hydrocarbons from highly porous chalk fields of the North Sea led to concerns about their strength in relation to possible pore collapse and reservoir compaction (*e.g.* Andersson *et al*. 1985; Ruddy *et al*. 1989; Hermansen *et al*. 1996). Andersson *et al*. (1985) cited rock mechanical experimental results which indicate that pore collapse can happen at 0.7% elastic strain in a chalk of 40% porosity. They then turned their focus to the quite significant correlation between strength and porosity, so consequently results from rock mechanical tests and seismic data are typically interpreted in terms of stress and porosity (*e.g.* Ruddy *et al*. 1989; Bredesen *et al*. 2021). Strength can be defined as the stress attained before pore collapse, and strength of chalk has been found to not only depend on porosity, but also on induration (cementation), and saturating fluids (*e.g*. Nermoen *et al*. 2018), but this finding may be a complicated way to predict the onset of collapse caused by stress: Because calcite constitutes the supporting frame in chalk, it would be a simple assumption, that for a given stress

geometry, irrespective of porosity and cementation, pore collapse would happen at a critical elastic strain of calcite, and consequently a similar elastic strain of the rock. Recent studies have indeed indicated that elastic strain at pore collapse is remarkably similar for different specimens and saturating fluids when tested under hydrostatic conditions, and also similar when tested under oedometer conditions (Meireles & Fabricius 2022; Proestakis *et al*. 2023; Orlander & Christensen 2024, 2025). The critical strain differs depending on stress geometry and was found to be higher for hydrostatic geometry where pervasive pore collapse takes place than for oedometric geometry where pore collapse takes place in the form of compaction bands (Orlander & Christensen 2024, 2025).

Orlander & Christensen (2025) did uniaxial strain tests on core samples of chalk from the Tuxen Formation, and because a core sample retrieved from burial contains microcracks caused by unloading, it is not simple, from mechanical strain data alone, to ascertain which part of the mechanical deformation is plastic (*i.e.* closure of cracks) and which part is elastic. Elastic waves are purely elastic, so when the tests are monitored by elastic waves, elastic moduli, Biot's coefficient and elastic strain can be calculated throughout the test according to the procedure of Gram *et al*. (2021), and then plastic strain due to closure of microcracks can be quantified. In this way, Orlander & Christensen (2025) found the onset of pore collapse to be at markedly constant uniaxial elastic strain (0.20–0.24%) corresponding to *c.* 0.45% volumetric strain, across samples with different porosity and different induration, and even with different saturating fluid. For this reason, we find it relevant to present a simple method to derive the *in situ* elastic strain of a formation using petrophysical logging data (Fabricius & Omdal 2021).

Theory

Most North Sea chalk fields are presently buried to an effective stress of more than 10 MPa, and the chalk accordingly will expand and contain unloading fractures when retrieved in cores. The mechanism behind the formation of unloading fractures is described by *e.g*. Santamarina (2001). They arise because the stress field during burial has a dominating vertical component, whereas during exhumation the stress field transits via hydrostatic to have dominating lateral components. This causes extensional horizontal microcracks and fractures. Because the stress field during burial is uniaxial, samples for rock mechanical testing are as a rule cut as vertical cylinders, and when loaded with a stress, σ_v under uniaxial strain conditions, a part of the total strain will reflect the closure of microcracks. Under hydrostatic stress, σ_H, total strain will also include closure of microcracks. To overcome the ambiguity caused by microcracks, the elastic strain during a test can be derived by monitoring total strain, ε_t and elastic wave velocities (v_P and v_S). First step is to calculate sample porosity, ϕ, and bulk density, ρ_b:

$$\phi = (\phi_o - \varepsilon_t)/(1- \varepsilon_t), \quad (1)$$

$$\rho_b = \rho_g (1- \phi) + \rho_{pf} \phi, \quad (2)$$

where ϕ_o is initial porosity, ρ_g is grain density, and ρ_{pf} is density of the pore fluid.

Next step is to calculate elastic moduli (*e.g*. Mavko *et al*. 2009):

$$\text{Shear modulus, } G = \rho_b v_S^2, \quad (3)$$

$$\text{P-wave modulus, } M = \rho_b v_P^2, \quad (4)$$

$$\text{Bulk modulus, } K = M - 4G/3. \quad (5)$$

The uniaxial, ε_M, and bulk, ε_K, elastic strain can be calculated:

$$\varepsilon_M = \sigma_v/M, \quad (6)$$

$$\varepsilon_K = \sigma_H/K. \quad (7)$$

The reasoning is now that the elastic strain measured from velocities in the laboratory will correspond to elastic strain derived from well logs *in situ*. This is justified by the finding that elastic waves in chalks are in the low frequency regime (Biot 1956) for frequencies up to 1 MHz (Fabricius *et al*. 2010), *i.e.* well above the logging frequency (20-35 kHz) and laboratory frequency (300 kHz and 600 kHz, for respectively P- and S-waves). We thus infer that there is a robust basis for implementing rock mechanical data to *in situ* conditions, where well logs can give information on ϕ, ρ_b, v_P and v_S, so that elastic moduli can be calculated. Vertical effective *in situ* stress, σ_v', can be estimated from depth, d, density of overburden, ρ_{ob}, the acceleration of gravity, g, and pore pressure, P:

$$\sigma_v' = g\, d\, \rho_{ob} - aP, \quad (8)$$

where a is Biot's coefficient (Biot & Willis 1957):

$$a = 1 - K_{fr}/K_{min}. \quad (9)$$

Bulk modulus of the mineral K_{min} is derived from tabulated data, or via the method presented by

Meireles & Fabricius (2023). When the bulk modulus of the pore fluid, K_{fl} can be assessed, bulk modulus of the mineral frame K_{fr} can be modelled by using Gassman's equation (Gasmann 1951):

$$\frac{K}{K_{min}-K}=\frac{K_{fr}}{K_{min}-K_{fr}}+\frac{K_{fl}}{\phi\left(K_{min}-K_{fl}\right)} \qquad (10)$$

Geological setting

The Valdemar field is located in the Danish sector of the central North Sea. It is over-pressured and unlike most reservoirs in the Danish Central Graben, the Valdemar field mainly hosts hydrocarbons in the Lower Cretaceous Tuxen and Sola formations, although hydrocarbons are also produced from the Upper Cretaceous chalks (Danish Energy Agency 2013). The western part of the Valdemar field is dominated by an elongated N-S structure that presents two structural highs (in this study represented by respectively Valdemar-2H and Bo-2X) separated by a saddle point (Fig. 1). In the eastern part of the field, a separate dome structure hosting hydrocarbons remains undeveloped (represented by Boje-2C). The geological setting and sedimentology of the Valdemar Field have been studied by several authors (*e.g.* Jakobsen *et al*. 2004, 2005; Ineson *et al*. 2022a, 2022b; Jelby *et al*. 2022). The studied formations comprise interbedded chalk, slightly marly chalk, marly chalk, chalky marlstones, marlstones and shale (Fig. 2). Blok *et al*. (2023) studied the clay mineralogy of these formations and found kaolinite to dominate (average content around 50%) followed by illite, mixed layer illite/smectite and chlorite. Pyrite content is low (0-5%) but can play a role in electrical conductivity (Storebø *et al*. 2022). Due to the varied lithology, water saturation varies significantly downhole. In combination with some questionable early downhole formation-tester pressure data, this has caused the belief that the reservoir is compartmentalized stratigraphically (Jakobsen *et al*. 2005; Glad *et al*. 2022), but a more detailed analysis indicates pore pressure equilibrium between Sola and Tuxen formations in a given structure (Fabricius *et al*. 2005).

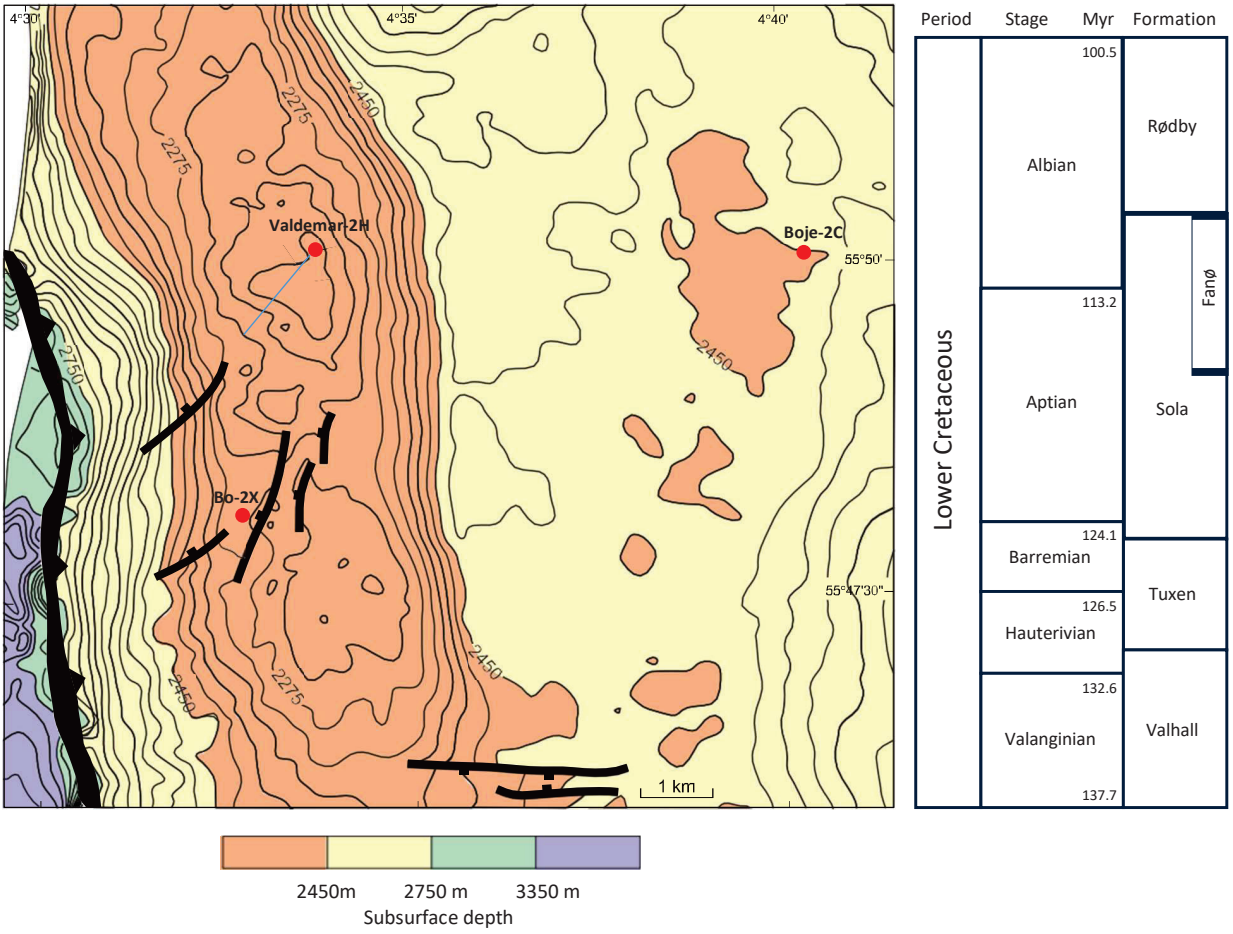
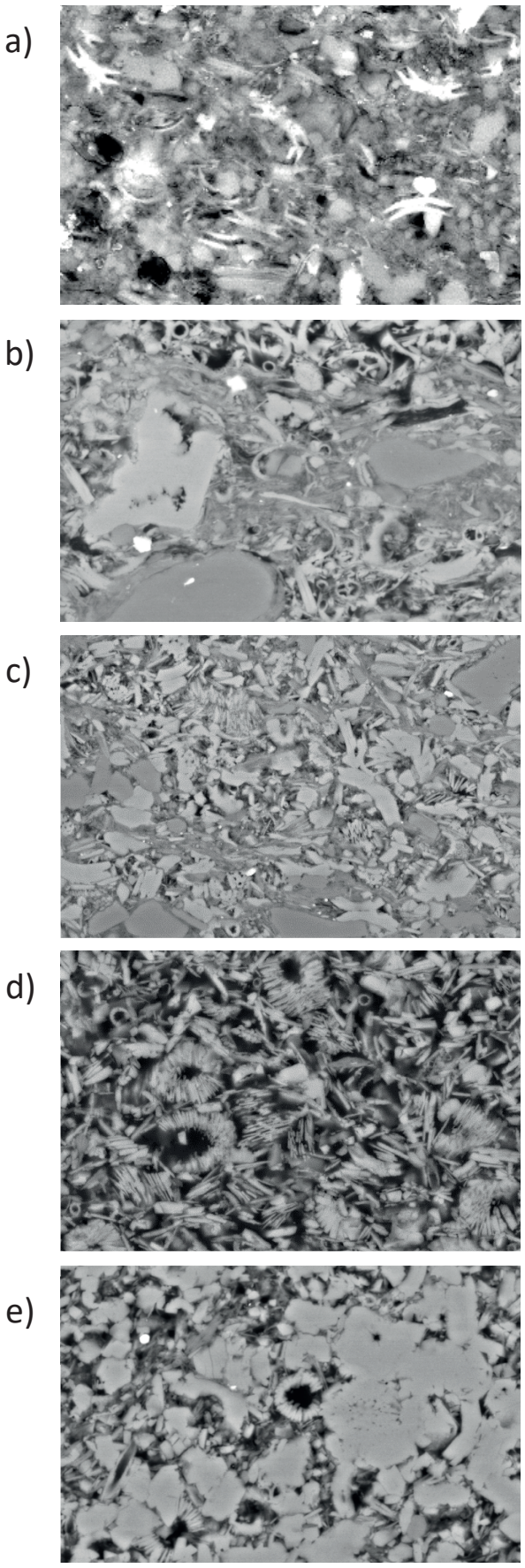


Fig. 1. (a) Structure map of the Lower Cretaceous Tuxen Formation (modified after Jakobsen *et al.* 2004) (b) Stratigraphic column (modified after Jelby *et al*. 2022).



Methodology

Downhole vertical elastic deformation is calculated from well logs covering the Lower Cretaceous Cromer Knoll Group, comprising Valhall, Tuxen, Sola and Rødby formations of wells Bo-2X, Valdemar-2H, and Boje-2C (Fig. 3), bottomhole temperature recorded was respectively; 83ºC, 80ºC, and 95ºC. Pore pressure data were available from the downhole formation tester tool of Bo-2X and Boje-2C. The data indicate an overpressure of 3 MPa in Bo-2X and of 9 MPa in the deeper Boje-2C. No pressure data are available for Valdemar-2H, but because this well is located in the same structure as Bo-2X, a similar overpressure is assumed (Fig. 1).

The caliper log indicates that the holes in Bo-2X and Boje-2C are practically in gauge, while the close to horizontal hole of Valdemar-2H is rough, in the sense that intervals with high natural gamma ray signal tend to have high diameter. The natural gamma ray log fluctuates as a reflection of varying content of radioactive clays, but in general, calcite is the loadbearing phase (Meireles & Fabricius 2023). The natural gamma ray log was used for estimating solid volume fraction of calcite, V_c, and of noncarbonates, V_{ir}.

All wells have deep (R_t) as well as medium (R_m) resistivity information. Boje-2C was drilled with oil-based mud, and mud filtrate invasion causes no discernable difference between the deep and medium resistivity logs. Bo-2X and Valdemar-2H were drilled with water-based mud, and whereas only a small split between the two resistivity-curves is seen for well Bo-2X, a significant split between the two curves is seen in Valdemar 2H. This can reflect mud filtrate invasion or be caused by the rough hole. The neutron porosity log was compared to the density log on an equivalent limestone porosity scale. The two logs indicate no marked effect of hydrocarbons. They are close where the natural gamma radiation is low and deviate where natural gamma radiation is high, so that a high clay content is indicated by a high neutron porosity. The bulk density log and medium resistivity logs were used for iterative calculation of near wellbore water saturation and porosity (S_{xo} and ϕ) by using grain density, ρ_g, derived from core data:

Fig. 2. Backscatter electron micrographs. **a**) Upper Sola Formation, Valdemar-1P, 7295 ft ss. Mixed sediment of clay, coccoliths and silt. **b**) Lower Sola Formation, Boje-2C, 8220 ft ss. Laminated carbonate ooze and clay with silt and shell fragments. **c**) Upper Tuxen Formation, Boje-2C, 8256 ft ss. Laminated carbonate ooze, clay and silt. **d**) Middle Tuen Formation, Valdemar-2H, 7568 ft ss. Massive carbonate ooze with nannoconids. **e**) Lower Tuxen Formation, Boje-2C, 8442 ft ss. Clay bearing chalk with recrystallized calcite.

$$\phi = (\rho_g - \rho_b)/(\rho_g - \rho_{pf}), \quad (11)$$

$$S_{xo} = (R_w/(\phi^{\,m} R_m))^{1/n}, \quad (12)$$

$$\rho_{pf} = \rho_w S_{xo} + (1 - S_{xo})\rho_{hc}. \quad (13)$$

Based on service company special core analysis data involving measurements of electrical conductivity of chalk samples saturated with systematically varying salinity of saturating brine and hydrocarbon content, the porosity exponent, m, was set to 2.02 for Bo-2X and Valdemar-2H, and to 2.00 for Boje-2C, similarly

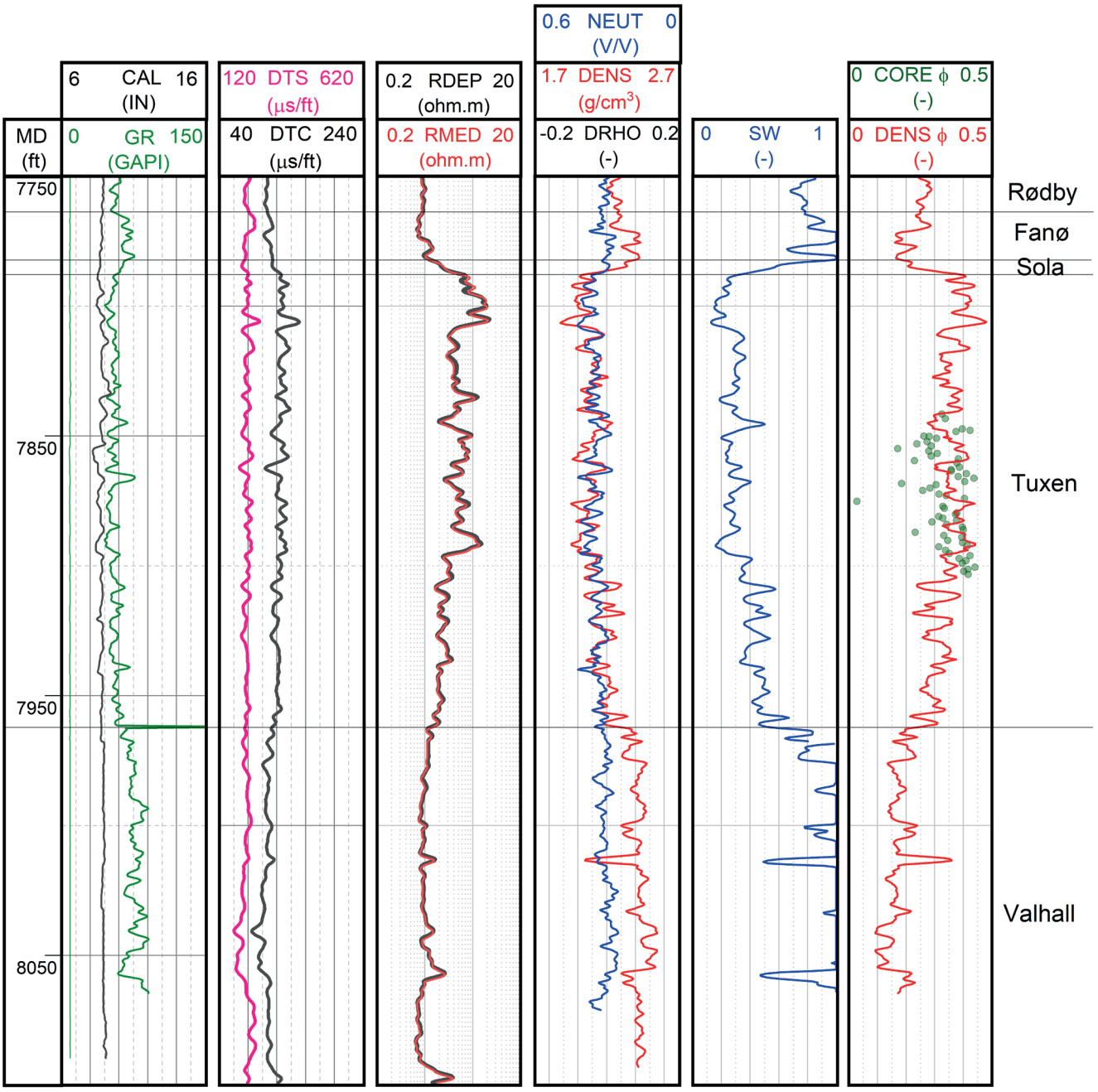


Fig. 3. Petrophysical downhole logs. **a**) Bo-2X (2307 m – 2407 m sub sea level). **b**) Valdemar-2H (horizontal: 2179–2273 m sub sea level). **c**) Boje-2C (2456–2578 m sub sea level). CAL: Borehole diameter (inches) measured by caliper; GR: Natural gamma ray radiation intensity measured in API units; DTS: Travel time (slowness) of elastic shear waves measured in microseconds per foot; DTC: Travel time (slowness) of elastic compressional waves measured in microseconds per foot; RDEP: Deep electrical resistivity measured in Ωm; RMED: Medium electrical resistivity measured in Ωm; NEUT: Neutron porosity calibrated in limestone, volume fraction V/V; DENS: Bulk density measured by gamma ray attenuation; DRHO: tool-indicated uncertainty on density reading; SW: modelled water saturation; Porosity, ϕ, from core data (CORE) and as calculated from density log (DENS).

the saturation exponent, n, was set to 2.11 for Bo-2X and Valdemar-2H, and to 2.00 for Boje-2C. Resistivity of pore water, R_w was estimated from temperature and pore water salinity (30.000 ppm for Bo-2X and Valdemar-2H and 100.000 ppm for Boje-2C). Water density, ρ_w, and bulk modulus, K_w, were estimated from salinity, temperature and pressure (Batzle & Wang 1992, as cited in Mavko *et al*. 2009). Hydrocarbon density, ρ_{hc}, and bulk modulus, K_{hc}, were estimated from production data, pressure and temperature. The water saturation, S_w, was then calculated from:

$$S_w = (R_w/(\phi^m R_t))^{1/n}. \quad (14)$$

The water saturation was found to be relatively low

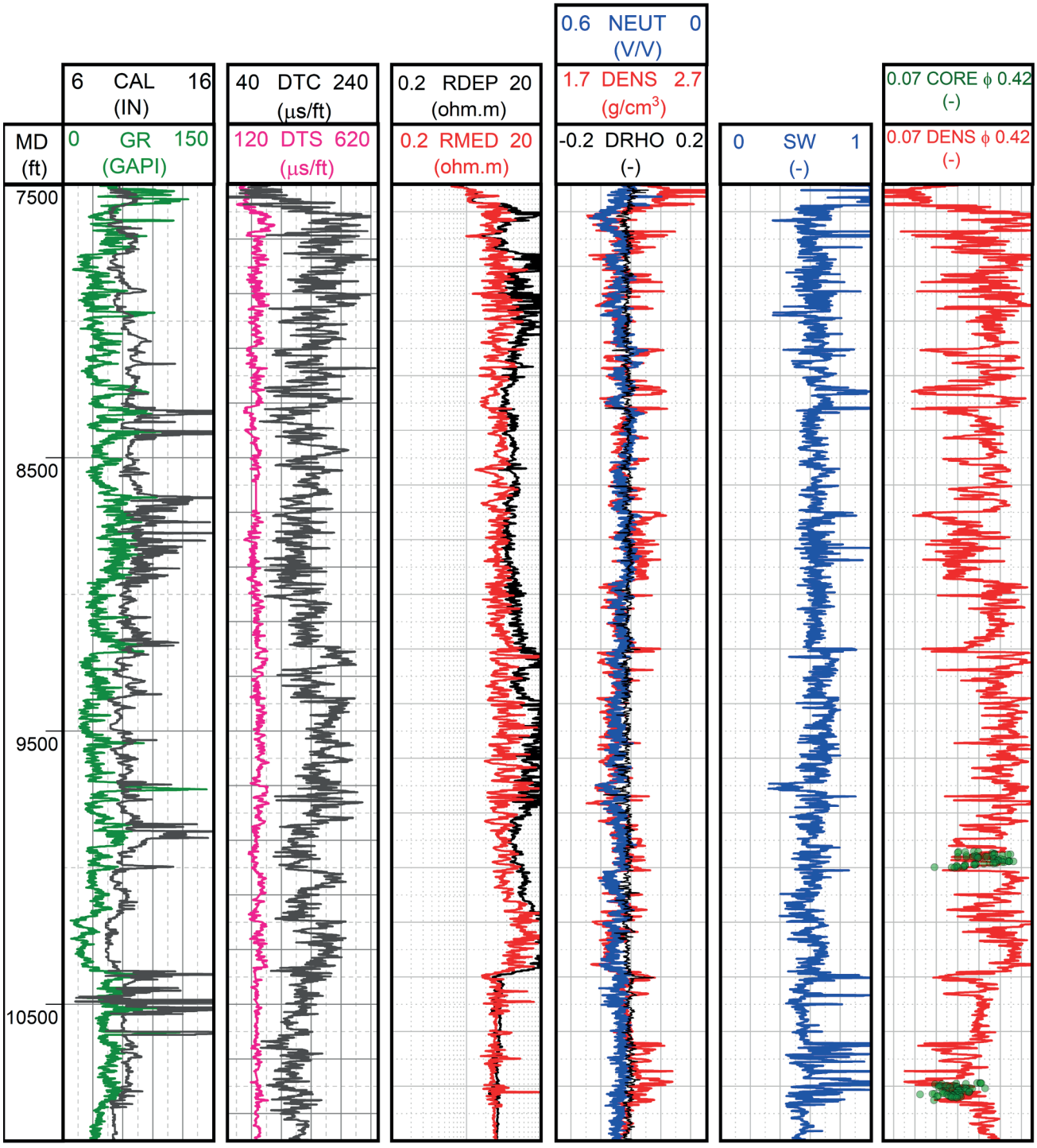


Fig. 3b. Valdemar-2H.

(S_w = 0.25) in the upper 100 ft of the Tuxen Formation of Bo-2X but increases to S_w = 0.6 near the transition to Valhall Formation. Bearing in mind the high and highly variable specific surface of these clay-rich chalks, these saturations would both correspond to irreducible water saturation (Fabricius *et al*. 2005). The high water saturation of Valdemar-2H is probably the effect of moderate clay content and can well be irreducible. In the Tuxen Formation of Boje-2C in the eastern structure, S_w increases depth-wise from 0.4 to 1.0, probably reflecting a transition to the water zone.

In situ P-wave modulus, *M*, and bulk modulus, *K*, were directly calculated from logging data (equations 3-5), whereas bulk modulus of the pore fluid, K_{fl}, and bulk modulus of the mineral phase, K_{min}, depend on component values. Both can be estimated as softest and stiffest mixtures, according to Reuss and Voigt bounds (Mavko *et al*. 2009):

$$1/K_{fl} = S_w/K_w + (1-S_w)/K_{hc}, \text{ or} \quad (15)$$

$$K_{fl} = S_w K_w + (1-S_w) K_{hc}, \text{ and} \quad (16)$$

$$1/K_{min} = V_c/K_c + (V_{ir})/K_{ir}, \text{ or} \quad (17)$$

$$K_{min} = V_c K_c + (V_{ir}) K_{ir}. \quad (18)$$

This allows a softest and stiffest estimate of K_{fr}. The bulk modulus of calcite, K_c, was set to 71 GPa, in accordance with citations in Mavko *et al*. (2009). Bulk modulus of the non-carbonate fraction, K_{ir}, was mod-

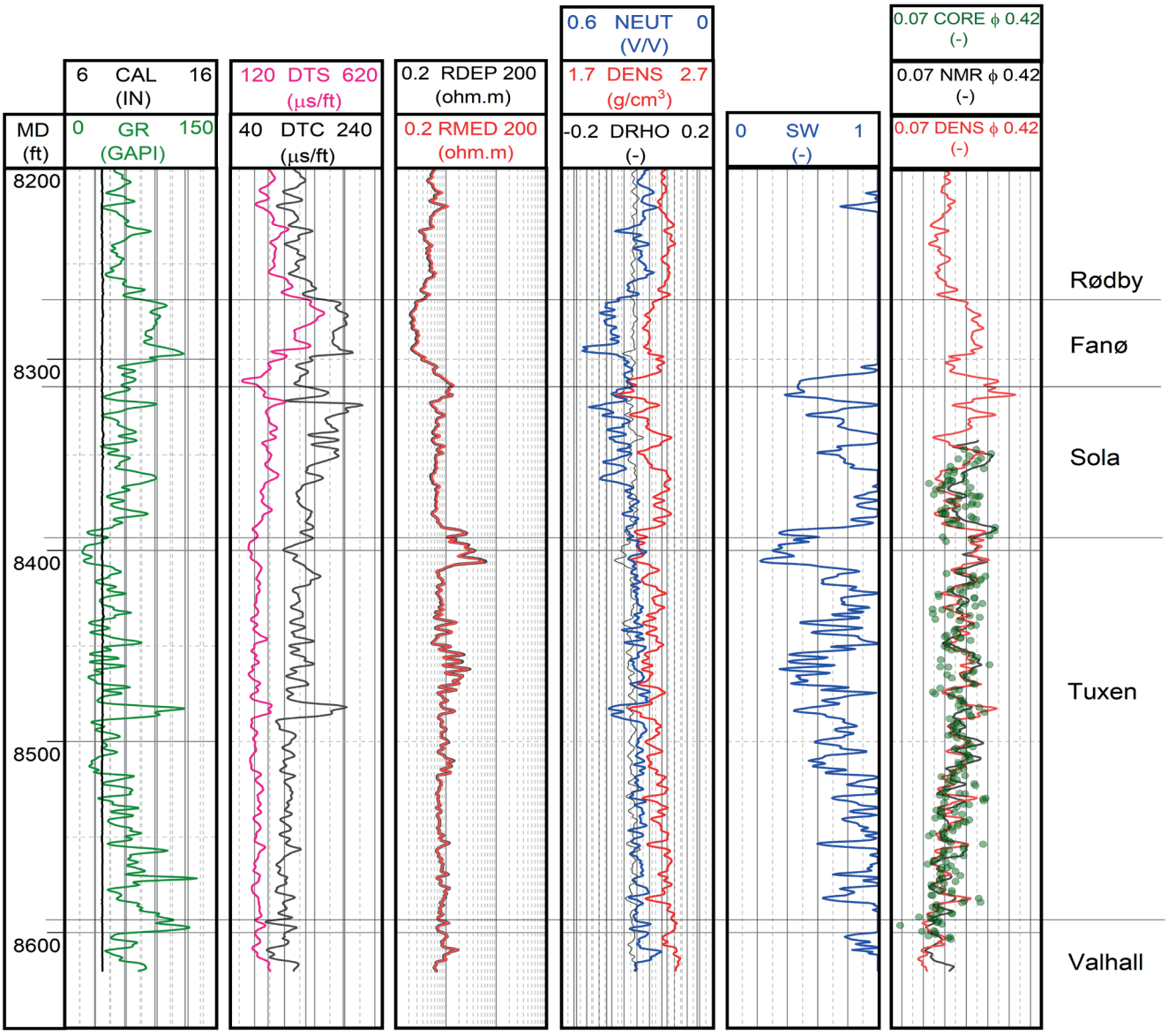
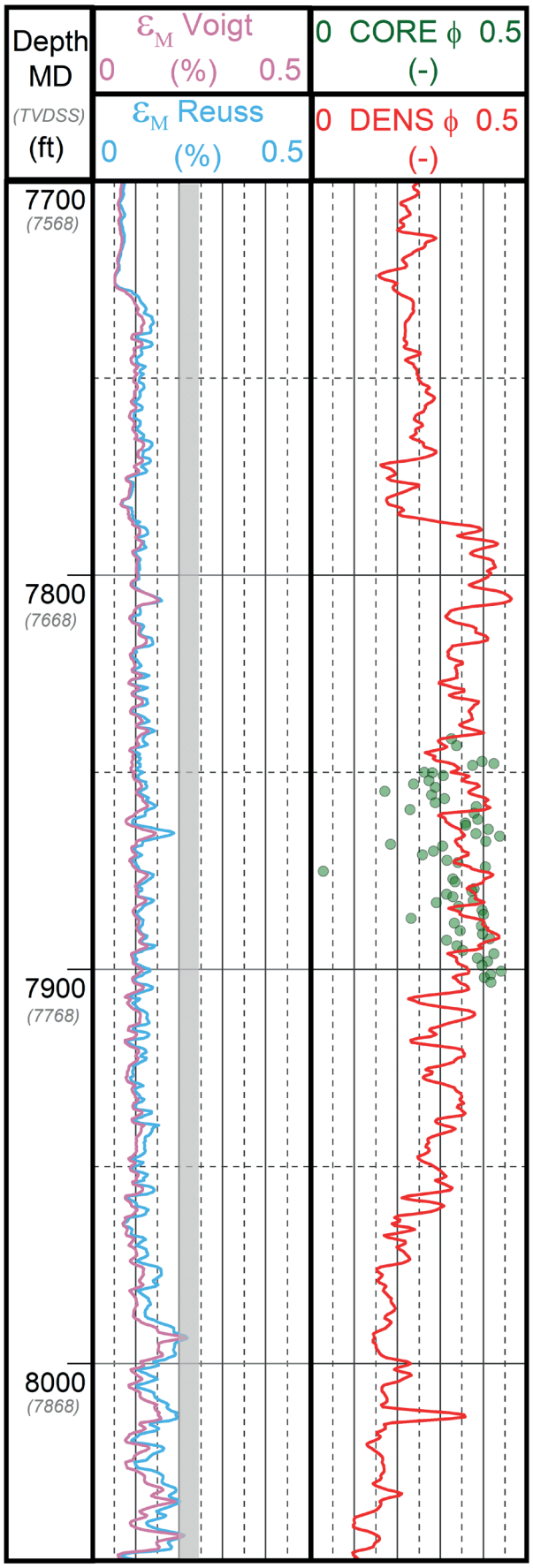


Fig. 3c. Boje-2C.



elled according to the method of Meireles & Fabricius (2023). Gassmann's equation (10) was used for the estimate of bulk modulus of the frame, K_{fr}, and Biot's coefficient, a was calculated from equation (9).

In situ vertical effective stress, σ_v', was calculated from equation (8). Data on vertical depth below sea level, d, were available for all wells (Figure 4) and the acceleration of gravity was set to 9.81 m/s^2. The average density of the overburden was set to 2.00 g/cm^3. The vertical *in situ* elastic strain can now be estimated from:

$$\varepsilon_M = \sigma'/M. \quad (19)$$

Results and discussion

Resulting porosity and elastic strain curves (Fig. 4) indicate that *in situ* elastic strain falls in the range 0.05% to 0.25%, which is relatively high as compared to typical Upper Cretaceous Chalk (Fabricius 2020). The calculated strain reflects a sediment with contact cementation but little pore filling cementation as a reflection of the absence of observed stylolites (Glad *et al*. 2022). The stiffest and softest choice of mixing of minerals and of pore fluids (Voigt and Reuss) do not give significantly different results. It should be noted though, that the difference between the Voigt and Reuss bounds is largest when near equal amounts of two components are mixed (non-carbonate and calcite, or oil and water; refer to equations 15–18).

For Bo-2X, elastic *in situ* strain was found to be relatively constant around 0.1% in the Tuxen Formation, whereas it alternates between 0.1% and 0.2% in the underlying Valhall Formation. The higher strain represents intervals with relatively high natural GR radiation reflecting high content of clay, where integrated contact area between calcite crystals is smaller and stress accordingly higher. Similarly, for Valdemar-2H, elastic *in situ* strain is rather constant and close to 0.1% as a reflection of the well being drilled horizontally in an interval with moderate clay content. In Boje-2C with higher overpressure (9 MPa *vs*. 3 MPa) and consequent lower effective stress in spite of deeper level, the situation is different: In the modestly clay-bearing Rødby and Sola formations and the underlying relatively clay poor Tuxen Formation, *in situ* strain is generally below 0.1% in the

Fig. 4. Modelled elastic strain logs, where critical strain is marked by grey box. **a**) Bo-2X (2307–2407 m subsea level). **b**) Valdemar-2H (horizontal: 2179–2273 m sub sea level). **c**) Boje-2C (2456–2578 m sub sea level). The *in situ* vertical uniaxial strain, ε_M, was modelled from *in situ* vertical effective stress and stiffness of rock and fluid components mixed in stiffest (Voigt) and softest (Reuss) way. Porosity, ϕ, from core data (CORE) and as calculated from density log (DENS).

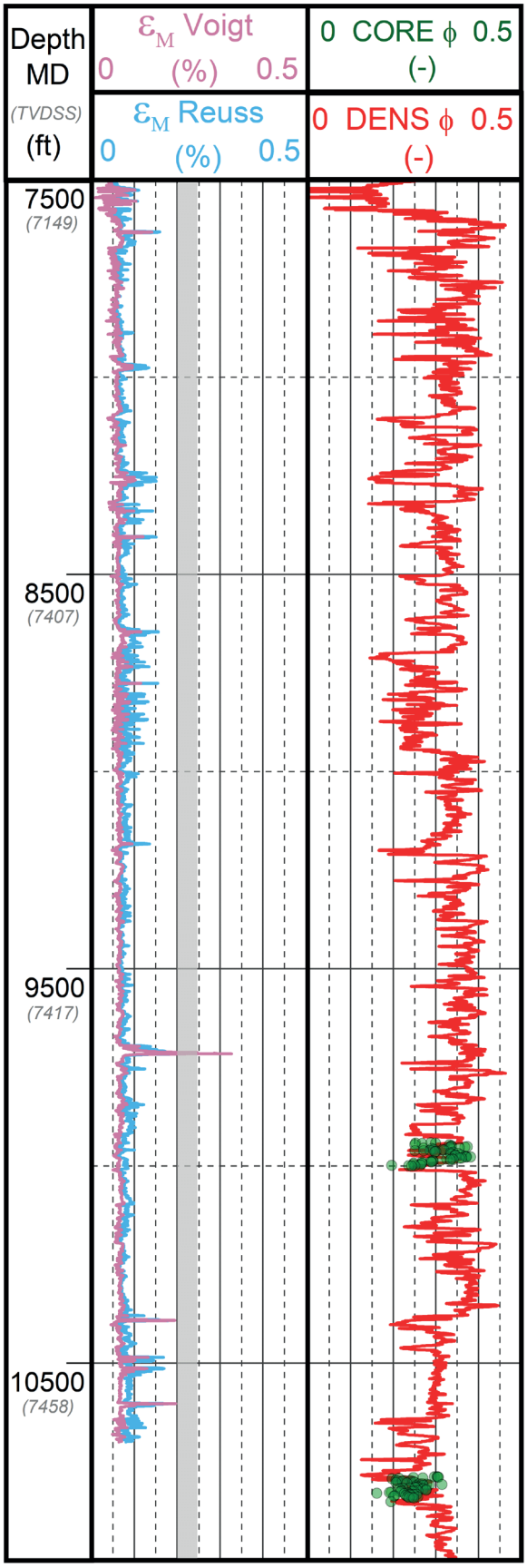


Fig. 4b. Valdemar-2H.

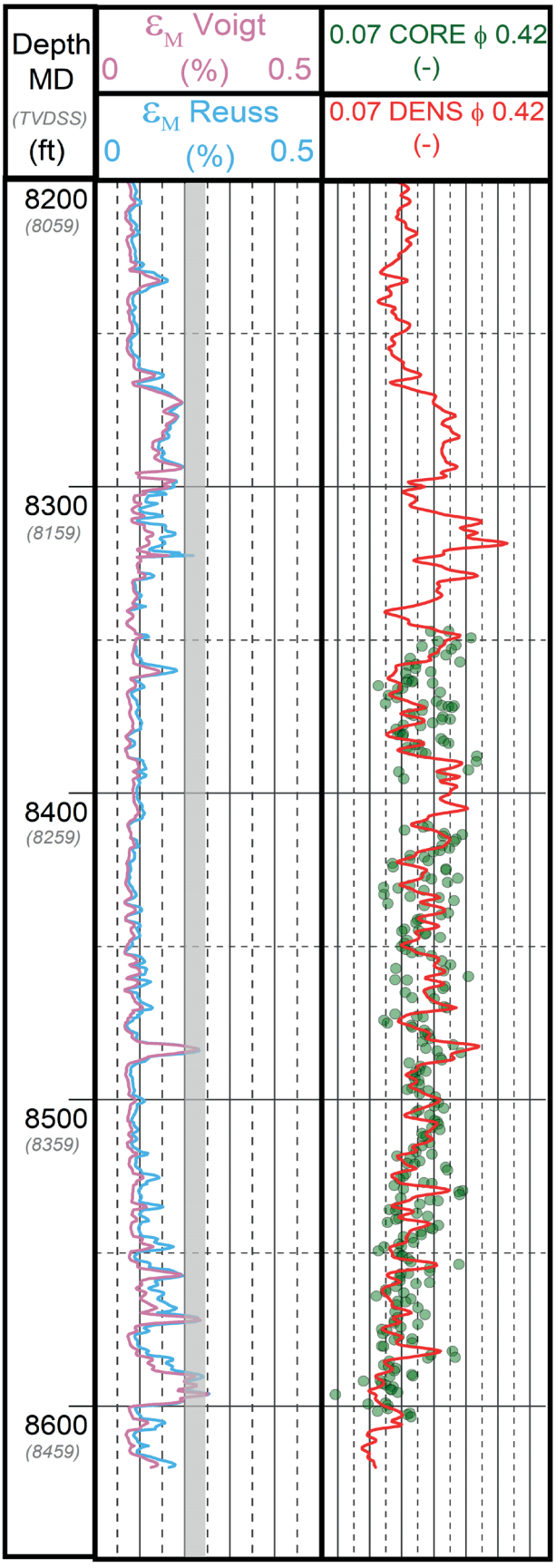


Fig. 4c. Boje-2C.

upper part but increases with depth as clay content and water saturation increases, and in single beds is estimated to exceed 0.3%. In the clay-rich Fanø Member in situ strain is modelled to approach 0.3%. In situ strain higher than critical strain according to Orlander & Christensen (2025; 0.20–0.24%) is thus generally found outside potential reservoir intervals.

The analyzed data are recorded pre-production, so falling pore pressure due to production could change this picture. For example, in wells from Ekofisk field, 20 years of production led to an increase in modelled *in situ* strain from 0.2% to 0.4% (Fabricius & Omdal 2021).

For Boje-2C the present vertical stress is around 50 MPa, and the pore pressure 34 MPa including 9 MPa over-pressure. For an interval with M = 12.5 GPa, this corresponds to an in situ strain of 0.13%, and if all over-pressure were released, to an in situ strain of 0.2%, close to the critical interval for pore collapse. For the two western wells in the Valdemar field, present vertical stress is around 45 MPa, and pore pressure is 26 MPa including 3 MPa overpressure. For an interval with M = 12.5 GPa, this corresponds to an in situ strain of 0.13%, and if all overpressure were released, to an in situ strain of 0.15%, apparently safely below the critical strain for pore collapse. For the Valdemar field the presented method thus allows us to identify pore-collapse-susceptible zones that could fail during depletion of the reservoir. This could inspire improving completion design, planned trajectory of infill wells, as well as abandonment practices. It should be borne in mind that the present approach assumes a stress field corresponding to uniaxial strain, so results should not be seen as more than an indication. More reliable results would require geomechanical modelling based on more detailed stress field information.

Conclusion

We have presented a method that allows us to model *in situ* elastic vertical strain from geophysical bore hole data. This is highly relevant for predicting potential for pore collapse in fragile reservoirs as chalk. The results are compared with experimental data which indicate that for a given stress-geometry, the onset of pore collapse in a given sedimentary rock is governed by a single critical elastic strain, irrespective of porosity and saturating pore fluid.

The analysed data represent the Lower Cretaceous chalk of Valdemar field and were recorded prior to production. At that stage the *in situ* strain was relatively low, and even if all over-pressure were relieved, no critical strain is to be anticipated in Bo-2X and Valdemar-2H. By contrast, if Boje-2C, where pore overpressure is higher, were put in production and all over-pressure released, reservoir intervals that presently have an *in situ* strain above 0.13%, would come near the critical strain of 0.2%.

Acknowledgements

We gratefully acknowledge the Danish Underground Consortium (TotalEnergies E&P Denmark, Noreco and Nordsøfonden) for granting permission to publish this work. The study was funded by the Danish Offshore Technology Centre (DTU Offshore). Morten Leth Hjuler is thanked for recording backscatter electron micrographs. Helle Foged Christensen and an anonymous referee are thanked for critical reviews of an earlier version of this paper.

References

Anderson, R.A., Edwards, D.P. & Ormerod, L. 1985: Log interpretation techniques to evaluate formation collapse in the North Sea chalk. Paper for Symposium of North Sea Chalk, sponsored by the Norwegian government, Stavanger, Norway, 21–22 May 1985, 1–20.

Batzle, M. & Wang, Z. 1992: Seismic properties of pore fluids. Geophysics 57, 1396–1524. https://doi.org/10.1190/1.1443207.

Biot, M.A. 1956: Theory of propagation of elastic waves in a fluid-saturated porous solid. I. Low-frequency range. The Journal of the Acoustical Society of America 28, 168–178. https://doi.org/10.1121/1.1908239

Biot, M.A. & Willis, D.G. 1957: The elastic coefficient of the theory of consolidation. Journal of Applied Mechanics 24, 594–601. https://doi.org/10.1115/1.4011606

Blok, C.N., Adatte, T., Ineson, J.R., Sheldon, E., Jelby, M.E., Smit, F.W.H., Lauridsen, B.W., Anderskouv, K. & Bodin, S. 2023: Clay mineral assemblages as a tool in source-to-sink studies: an example from the Lower Cretaceous of the North Sea Basin. Bulletin of the Geological Society of Denmark 71, 99–113. https://doi.org/10.37570/bgsd-2023-71-06

Bredesen, K., Lorentzen, M., Nielsen, L. & Mosegaard, K. 2021: Quantitative seismic interpretation of the Lower Cretaceous reservoirs in the Valdemar Field, Danish North Sea. Petroleum Geoscience 27, 1–17. https://doi.org/10.1144/petgeo2021-016

Danish Energy Agency 2013: Oil and gas production in Denmark 2013 and subsoil use, 105 pp. Copenhagen: Energistyrelsen.

Fabricius, I.L., Olsen, C. & Prasad, M. 2005: Log interpretation of marly chalk, the Lower Cretaceous Valdemar Field, Danish North Sea. Application of iso-frame and pseudo water film concepts. The Leading Edge 24, 449–560. https://doi.org/10.1190/1.1926807

Fabricius I.L., Bächle, G.T. & Eberli, G.P. 2010: Elastic moduli of dry and water-saturated carbonates – effect of depositional texture, porosity, and permeability. Geophysics 75, 65–78. https://doi.org/10.1190/1.3374690

Fabricius I.L. 2020: Porosity in chalk – roles of elastic strain

and plastic strain. Sedimentology 67, 3451–3470. https://doi.org/10.1111/sed.12750

Fabricius, I.L. & Omdal, E. 2021: Elastic strain of chalk due to oil production. Biot-Bažant Conference, June 1–3, 2021, Northwestern University, Evanston, IL.

Gassman, F. 1951: Über die Elastizität poröser Medien. Vierteljahrsschrift der Naturforschenden Gesellschaft in Zürich 96, 1–23.

Glad, A.C., Amour, F., Welch, M.J., Clausen, O.R., Anderskouv, K. Ineson, J.R., Sheldon, E. & Nick, H.M. 2022: Natural fractures and discontinuities in a Lower Cretaceous chalk-marlstone reservoir, Valdemar Field, Danish North Sea. Marine and Petroleum Geology 136, 1–15. https://doi.org/10.1016/j.marpetgeo.2021.105445

Gram, T.B., Ditlevsen, F.P., Mosegaard, K. & Fabricius, I.L. 2021: Water-flooding and consolidation of reservoir chalk – effect on porosity and Biot's coefficient. Geophysical Prospecting 69, 495–513. https://doi.org/10.1111/1365-2478.13047

Hermansen, H., Thomas, L.K., Sylte, J.E. & Aasbøe, B.T. 1997: Twentyfive years of Ekofisk reservoir management. Presented at the Annual Technical Conference and Exhibition, San Antonio, Texas, 5–8 October. SPE-38927. https://doi.org/10.2118/38927-ms

Ineson, J.R., Petersen, H.I., Andersen, C., Bjerager, M., Jakobsen, F.C., Kristensen, L., Mørk, F. & Sheldon, E. 2022a: Early Cretaceous stratigraphic and basinal evolution of the Danish Central Graben: a review: Bulletin of the Geological Society of Denmark 71, 75–98. https://doi.org/10.37570/bgsd-2022-71-05

Ineson, J.R., Lauridsen, B.W., Lode, S., Sheldon, E., Sørensen, H.O., Wisshak, M. & Anderskouv, K. 2022b: A condensed chalk–marl succession on an Early Cretaceous intrabasinal structural high, Danish Central Graben: Implications for the sequence stratigraphic interpretation of the Munk Marl Bed. Sedimentary Geology 440, 106234, 1–24. https://doi.org/10.1016/j.sedgeo.2022.106234

Jakobsen, F., Ineson, J.R. Kristensen, L. & Stemmerik, L. 2004: Characterization and zonation of a marly chalk reservoir: the Lower Cretaceous Valdemar Field of the Danish Central Graben. Petroleum Geoscience 10, 21–33. https://doi.org/10.1144/1354-079303-584

Jakobsen, F., Ineson, J.R., Kristensen, L., Nytoft, H.P. & Stemmerik, L. 2005: The Valdemar Field, Danish Central Graben: field compartmentalization and regional prospectivity of the Lower Cretaceous chalk play. In: Doré, A.G. & Vinning, B.A. (eds): Petroleum Geology: North-West Europe and Global Perspectives – Proceedings of the 6th Petroleum Geology Conference, 177–186. https://doi.org/10.1144/0060177

Jelby, M.E., Ineson, J.R., Thibault, N., Bodin, S., Blok, C.N., Edvardsen, N., Clemmensen, T.S., Buls, T. & Anderskouv, K. 2022: Facies and depositional processes of Lower Cretaceous carbonates, Danish Central Graben. Bulletin of the Geological Society of Denmark 71, 51–74. https://doi.org/10.37570/bgsd-2022-71-04

Mavko, G., Mukerji, T., and Dvorkin, J., 2009: Rock physics handbook: Tools for seismic analysis in porous media. Cambridge University Press. https://doi.org/10.1017/cbo9780511626753

Meireles, L.T.P. & Fabricius, I.L. 2022: Strain modeling in a marly chalk reservoir. In: Delgado-Martin, J., Muñoz-Ibañez, A. & Falcon-Suarez, I.H. (eds): 6th International Workshop on Rock Physics, A Coruña, Spain 13 –17 June 2022: Book of Abstracts, 53–54. https://doi.org/10.17979/spudc.000005

Meireles, L.T.P. & Fabricius, I.L. 2023: Deriving mineral moduli of the noncarbonate fraction in a marly chalk reservoir using petrophysical logging data and an isoframe model. Geophysics 88, D411-D425. https://doi.org/10.1190/geo2022-0493.1

Nermoen, A., Korsnes, R.I., Storm, E., Stodle, T., Madland, M.V. & Fabricius, I.L. 2018: Incorporating electrostatic effects into the effective stress relation – insights from chalk experiments. Geophysics 83, MR123-MR135. https://doi.org/10.1190/geo2016-0607.1

Orlander, T. & Christensen, H.F. 2024: Compaction phases and pore collapse in Lower Cretaceous chalk – insight from Biot's coefficient. Rock Mechanics and Rock Engineering. https://doi.org/10.1007/s00603-024-03963-x

Orlander, T. & Christensen, H.F. 2025: Elastic and plastic deformation of Lower Cretaceous North Sea Chalk during stress and time-dependent uniaxial strain compaction. Submitted to Rock Mechanics and Rock Engineering. https://doi.10.1007/s00603-025-04691-6

Proestakis, E., Christensen, H.F., Meireles, L.T.P., Storebø, E.M., Shamsolhodaei, A. & Orlander, T. 2023: Detection and picking of shear wave arrival for stiffness evaluation of highly porous chalk. Geophysical Prospecting 72, 733–751. https://doi.org/10.1111/1365-2478.13435

Ruddy, I., Andersen, M.A., Pattillo, P.D., Bishlawi, M. & Foged, N. 1998: Rock compressibility, compaction, and subsidence in a high-porosity chalk reservoir: A case study of Valhall Field. Journal of Petroleum Technology 41, 741–746, (SPE-18278-PA). https://doi.org/10.2118/18278-pa

Santamarina, J.C. 2001: Soil behavior at the microscale: Particle forces. Proc. Symp. Soil Behavior and Soft Ground Construction, in honor of Charles C. Ladd – October 2001, MIT, 31 pp. https://doi.org/10.1061/40659(2003)2

Storebø, E.M., Hjuler, M.L., Meireles, L.T.P. & Fabricius, I L. 2022: Effect of pyrite in water saturation evaluation of clay-rich carbonate. Petrophysics 63, 172–198. https://doi.org/10.30632/pjv63n2-2022a3